Analysis of Spatial Correlation with respect to Polarization and Pattern

Dao Manh Tuan(1) and Seong-Ook Park(1)
(1) Microwave and Antenna Laboratory, School of Engineering
Information and Communications University, Taejon, 305-732, Korea
E-mail: tuandm@icu.ac.kr, sopark@icu.ac.kr

Introduction

MIMO system, which can satisfy the demand of high capacity in wireless communications, has been paid much attention through years. Due to the fact that capacity of MIMO depends on the correlation between the waves impinging on two antenna elements, many studies on properties of the correlation have been widely carried out [1-4]. It has been shown that correlation depends on polarization, pattern of elements, spacing, and power azimuth spectrum (PAS). Close form of correlation and dependence of correlation on PAS and directive antenna are presented in [1], [2] and [3]. However, by assuming that patterns of all elements are identical or omidirectional, impact of patterns and polarization between elements on correlation is not considered. In this paper, we derive and analyze the spatial correlation with respect to polarization and pattern, based on a physically intuitional stochastic channel model for multiple-input multiple-output (MIMO) using polarized array. Simulations are performed using two dipoles with various configurations to investigate effects of polarization, patterns between elements. Results show that the correlation is very sensitive to orthogonality of pattern and polarization.

Polarized channel model and spatial correlation

Consider a MIMO system with N_T transmit and N_R receive antennas in Fig. 1, the input-output relationship can be expressed as

$$\mathbf{y}(t) = \mathbf{H}(t)\mathbf{x}(t) + \mathbf{n}(t) \quad (1)$$

where $\mathbf{y}(t)$, $\mathbf{x}(t)$, and $\mathbf{n}(t)$ denote transmitted signal vector, receive red signal vector and noise vector, respectively. $\mathbf{H}(t)$ is N_R x N_T complex channel coefficient matrix. Let us assume flat fading channel and NLOS propagation environment, $h_{qs}(t)$, the (q, s) component($q=1..N_R$, $s=1\ldots N_T$) of $\mathbf{H}(t)$, can be expressed as

$$h_{qs}(t)=\sum_{l=1}^{L}\left(A_l\begin{bmatrix}\sqrt{G_{TX,s}^{(v)}(\beta_l)}\\ \sqrt{G_{TX,s}^{(h)}(\beta_l)}\end{bmatrix}^T\begin{bmatrix}\exp\left(j\Phi_l^{(v,v)}\right) & \sqrt{\kappa_l}\exp\left(j\Phi_l^{(h,v)}\right)\\ \sqrt{\kappa_l}\exp\left(j\Phi_l^{(v,h)}\right) & \exp\left(j\Phi_l^{(h,h)}\right)\end{bmatrix}\begin{bmatrix}\sqrt{G_{RX,q}^{(v)}(\varphi_l)}\\ \sqrt{G_{RX,q}^{(h)}(\varphi_l)}\end{bmatrix}\times\right.$$
$$\left.\exp\left(jkd_s\sin(\beta_l+\theta_{TX})\right)\times\exp\left(jkd_q\sin(\varphi_l+\theta_{RX})\right)\times\exp\left(jk\|\mathbf{v}\|\cos(\varphi_l-\theta_v)t\right)\right) \quad (2)$$

where L is the number of sub-rays; A_l is the amplitude of the lth sub-ray; β_l and φ_l are the angle of departure and arrival of the lth sub-ray, respectively; $G_{TX,s}^{(v)}(\beta_l)$ and $G_{TX,s}^{(h)}(\beta_l)$ are the pattern of sth element in TX array for V and H polarization,

respectively; $G_{RX,q}^{(v)}(\varphi_l)$ and $G_{TX,q}^{(h)}(\varphi_l)$ are the pattern of sth element in RX array for V and H polarization, respectively; d_s is the distance between the sth element and the reference in TX array; d_q is the distance between the qth element and the reference in RX array; $\phi_l^{(v,v)}$, $\phi_l^{(v,h)}$, $\phi_l^{(h,v)}$ and $\phi_l^{(h,h)}$ are the phase offset of lth sub-ray for each of the four polarization channels VV, VH, HV and HH; κ_l is the inverse XPD value for VV/VH and HH/HV; θ_{TX} is the angle between the TX array broadside and the LOS direction; θ_{RX} is the angle between the RX array broadside and the LOS direction; θ_v is the angle between the velocity vector and the the RX array broadside and; **v** is the RX velocity vector.

The spatial correlation at RX between two paths impinging on two different RX antennas (q and r), but emanating from the same TX antenna (s), is expressed as [2]:

$$\rho_{qr}^{MS} = \frac{E\{h_{qs}(t)h_{rs}^*(t)\}}{\sqrt{E\{\left|h_{qs}(t)\right|^2\}}\sqrt{E\{\left|h_{rs}(t)\right|^2\}}} \tag{3}$$

where E{.} is the expectation operator.

$$E\{h_{qs}(t)h_{rs}^*(t)\} =$$

$$\sum_{l=1}^{L}\left\{E\{A_l^2\left|\beta_l,\varphi_l\right.\}E\left\{\begin{pmatrix}\begin{bmatrix}\sqrt{G_{TX,s}^{(v)}(\beta_l)}\\ \sqrt{G_{TX,s}^{(h)}(\beta_l)}\end{bmatrix}^T\begin{bmatrix}e^{j\phi_l^{(v,v)}}\sqrt{\kappa_l}\,e^{j\phi_l^{(h,v)}}\\ \sqrt{\kappa_l}\,e^{j\phi_l^{(v,h)}}\,e^{j\phi_l^{(h,h)}}\end{bmatrix}\begin{bmatrix}\sqrt{G_{RX,q}^{(v)}(\varphi_l)}\\ \sqrt{G_{RX,q}^{(h)}(\varphi_l)}\end{bmatrix}\end{pmatrix}\\ \begin{pmatrix}\begin{bmatrix}\sqrt{G_{TX,s}^{(v)}(\beta_l)}\\ \sqrt{G_{TX,s}^{(h)}(\beta_l)}\end{bmatrix}^T\begin{bmatrix}e^{-j\phi_l^{(v,v)}}\sqrt{\kappa_l}\,e^{-j\phi_l^{(h,v)}}\\ \sqrt{\kappa_l}\,e^{-j\phi_l^{(v,h)}}\,e^{-j\phi_l^{(v,v)}}\end{bmatrix}\begin{bmatrix}\sqrt{G_{RX,r}^{(v)}(\varphi_l)}\\ \sqrt{G_{RX,r}^{(h)}(\varphi_l)}\end{bmatrix}\end{pmatrix}\right\}e^{jkd\sin(\phi_l+\theta_{RX})}\right\} \tag{4}$$

where $d = d_q - d_r$ is the spacing between the element q and r; κ_l =1/XPD, XPD (in dB) ~ N(μ,σ), depending on propagation environment, μ varies from 0 to 18 dB, σ is in the order of 3-8 dB [4]; $\phi^{(v,v)}$, $\phi^{(v,h)}$, $\phi^{(h,v)}$ and $\phi^{(h,h)} \sim U[-\pi,\pi]$. $E\{A_l^2\left|\beta_l,\varphi_l\right.\}$ is the expected relative power conditioned on the azimuth angles of β_l and φ_l, and when $L \to \infty$ it can be expressed as

$$E\{A_l^2\left|\beta_l,\varphi_l\right.\} = P_A^{TX}(\beta)d\beta P_A^{RX}(\varphi)d\varphi \tag{5}$$

$P_A^{TX}(\beta)$ and $P_A^{RX}(\varphi)$ are power azimuth spectrum (PAS) at TX and RX respectively, they are assumed to be Laplacian distribution:

$$P_A(\beta) = \frac{1}{\sqrt{2}\sigma_A}e^{\frac{-\sqrt{2}}{\sigma_A}|\beta|} \qquad \beta \in [-\pi,\pi]. \tag{6}$$

After some mathematical transformations (not shown here due to the limitation of this paper), (4) becomes the following integral form:

$$E\{h_{qs}(t)h_{rs}^*(t)\} = \int_{-\pi}^{\pi}\int_{-\pi}^{\pi} P_A^{TX}(\beta)P_A^{RX}(\varphi)F_{qr}(\beta,\varphi)e^{jkd\sin(\varphi+\theta_{RX})}d\varphi d\beta \tag{7}$$

where

$$F_{qr}(\beta,\varphi) =$$

$$
\left\{
\begin{aligned}
&G_{TX,s}^{(v)}(\beta)\sqrt{G_{RX,q}^{(v)}(\varphi)G_{RX,r}^{(v)}(\varphi)}+\sqrt{G_{TX,s}^{(h)}(\beta)G_{RX,q}^{(v)}(\varphi)G_{TX,s}^{(v)}(\beta)G_{RX,r}^{(v)}(\varphi)}e^{\sigma^2\frac{1}{400}\ln^2 10-\mu\frac{1}{20}\ln 10}\\
&+G_{TX,s}^{(v)}(\beta)\sqrt{G_{RX,q}^{(h)}(\varphi)G_{RX,r}^{(v)}(\varphi)}e^{\sigma^2\frac{1}{400}\ln^2 10-\mu\frac{1}{20}\ln 10}+\sqrt{G_{TX,s}^{(h)}(\beta)G_{RX,q}^{(h)}(\varphi)G_{TX,s}^{(v)}(\beta)G_{RX,r}^{(v)}(\varphi)}\\
&+\sqrt{G_{TX,s}^{(v)}(\beta)G_{RX,q}^{(v)}(\varphi)G_{TX,s}^{(h)}(\beta)G_{RX,r}^{(v)}(\varphi)}e^{\sigma^2\frac{1}{400}\ln^2 10-\mu\frac{1}{20}\ln 10}+G_{TX,s}^{(h)}(\beta)\sqrt{G_{RX,q}^{(v)}(\varphi)G_{RX,r}^{(v)}(\varphi)}e^{\sigma^2\frac{1}{100}\ln^2 10-\mu\frac{1}{10}\ln 10}\\
&+\sqrt{G_{TX,s}^{(v)}(\beta)G_{RX,q}^{(h)}(\varphi)G_{TX,s}^{(h)}(\beta)G_{RX,r}^{(v)}(\varphi)}e^{\sigma^2\frac{1}{100}\ln^2 10-\mu\frac{1}{10}\ln 10}+G_{TX,s}^{(h)}(\beta)\sqrt{G_{RX,q}^{(h)}(\varphi)G_{RX,r}^{(v)}(\varphi)}e^{\sigma^2\frac{1}{400}\ln^2 10-\mu\frac{1}{20}\ln 10}\\
&+G_{TX,s}^{(v)}(\beta)\sqrt{G_{RX,q}^{(v)}(\varphi)G_{RX,r}^{(h)}(\varphi)}e^{\sigma^2\frac{1}{400}\ln^2 10-\mu\frac{1}{20}\ln 10}+\sqrt{G_{TX,s}^{(h)}(\beta)G_{RX,q}^{(v)}(\varphi)G_{TX,s}^{(v)}(\beta)G_{RX,r}^{(h)}(\varphi)}e^{\sigma^2\frac{1}{100}\ln^2 10-\mu\frac{1}{10}\ln 10}\\
&+G_{TX,s}^{(v)}(\beta)\sqrt{G_{RX,q}^{(h)}(\varphi)G_{RX,r}^{(h)}(\varphi)}e^{\sigma^2\frac{1}{100}\ln^2 10-\mu\frac{1}{10}\ln 10}+\sqrt{G_{TX,s}^{(h)}(\beta)G_{RX,q}^{(h)}(\varphi)G_{TX,s}^{(v)}(\beta)G_{RX,r}^{(h)}(\varphi)}e^{\sigma^2\frac{1}{400}\ln^2 10-\mu\frac{1}{20}\ln 10}\\
&+\sqrt{G_{TX,s}^{(v)}(\beta)G_{RX,q}^{(v)}(\varphi)G_{TX,s}^{(h)}(\beta)G_{RX,r}^{(h)}(\varphi)}+G_{TX,s}^{(h)}(\beta)\sqrt{G_{RX,q}^{(v)}(\varphi)G_{RX,r}^{(h)}(\varphi)}e^{\sigma^2\frac{1}{400}\ln^2 10-\mu\frac{1}{20}\ln 10}\\
&+\sqrt{G_{TX,s}^{(v)}(\beta)G_{RX,q}^{(h)}(\varphi)G_{TX,s}^{(h)}(\beta)G_{RX,r}^{(h)}(\varphi)}e^{\sigma^2\frac{1}{400}\ln^2 10-\mu\frac{1}{20}\ln 10}+G_{TX,s}^{(h)}(\beta)\sqrt{G_{RX,q}^{(h)}(\varphi_l)G_{RX,r}^{(h)}(\varphi)}
\end{aligned}
\right\} \quad (8)
$$

The denominator of (3) is solved in the same way, due to the limitation of this paper, the result is not shown here.

Simulation results and Discussion

The spatial correlation is simulated to study the effects of propagation environment, polarization and pattern of arbitrary antennas. For the sake of simplicity, the two elements (the qth and rth in the previous Section) of RX array are assumed to be half-wavelength dipole antennas which are depicted in Fig. 2. To study the impact of polarization on the spatial correlation, the qth element is fixed in the vertical plane and the rth element is rotated in the xz plane, with the slant angle of α, as shown in Fig. 2a. Fig. 3a shows the results of correlation different cases of the slant angle α. As can be seen, the higher slant angle, the lower the correlation, at the same spacing. Or the better polarization orthogonality, the lower the correlation. At the slant angle of 90^0, or completely polarized orthogonality, the correlation drops quickly, from 0.66 to 0.04, at the spacing less than 0.75 times of wavelength. To investigate effects of patterns on the spatial correlation, the two dipoles are horizontally placed in the xy plane as shown in Fig. 2b. The qth element is fixed while the rth element is rotated in the xy plane, with the rotation angle of ϕ. In Fig. 3b, we compare the spatial correlation for different rotation angles. The result shows that the correlation is very sensitive to rotation angle ϕ at small spacing between the two elements. The correlation is the lowest when $\phi = 90^0$, or when the two patterns are orthogonal, and it sharply increases when the orthogonality is not maintained. So it is possible to use pattern diversity as a means to create uncorrelated channels across elements.

Conclusions

This paper has derived and analyzed the spatial correlation based on stochastic channel model. Simulations are made using dipole antennas to study effects of polarization and patterns on spatial correlation. Results show that the correlation can be reduced by using polarization or pattern diversity and would be minimized if patterns or polarization of elements are orthogonal.

References

[1] Nokia, “BS correlation with antenna pattern”, SCM-098-NOK-Correlation.

[2] Laurent Schumacher, “Closed-Form Expressions for Correlations Coefficient of Directive Antennas Impinged by a Multimodal Truncated Laplacian PAS,” IEEE Trans. Commun., vol.4, no. 4, pp. 1351-1359, Jul. 2005.

[3] J. Li, E. Y. Zhang,” Analysis of the spatial correlation properties of wireless MIMO channel,” Proc. ISCIT2005, pp.214-217, 2005.

[4] M. Shafi, M. Zhang, A.L Moustakas, P.J. Smith, A.F. Molisch, F. Tufvesson, S.H. Simon, “Polarized MIMO channels in 3-D: models, measurements and mutual information, ” IEEE J. on Sele. Areas in Comm., vol. 24, no. 3, pp. 514-527, Mar. 2006.

[5] 3GPP, “Spatial channel model for MIMO simulations”, TR 25.996 V6.1.0. Sep. 2003. [Online]. Available: http://www.3gpp.org/

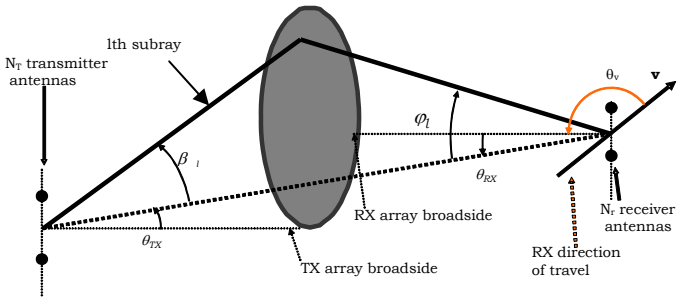

Fig 1. MIMO configuration under stochastic channel model

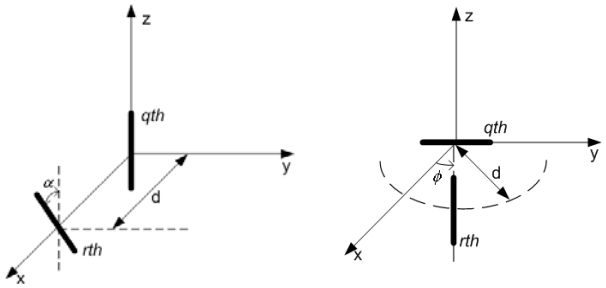

(a) (b)

Figure 2. Configuration of half-wavelength dipole antennas. (a) Two dipoles in the xz plane. (b) Two dipoles in the xy plane.

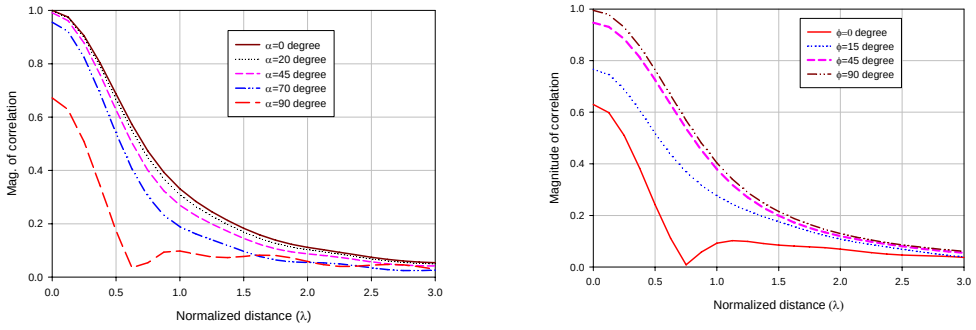

(a) (b)

Figure 3. Spatial correlation vs. spacing for different slant and rotation angles (a) Different slant angles. (b) Different rotation angles.